Oxidation behavior of H2 and CO produced by H2O and/or CO2 reduction in molten carbonates: Effect of gas environment and hydroxides

E. Gürbüz, V. Albin, V. Lair, A. Ringuedé, M. Cassir

Version of Record: https://www.sciencedirect.com/science/article/pii/S0013468621014924
Manuscript_f08d0b2156c11ade1b4dadb57d7afa4b

OXIDATION BEHAVIOR OF H_2 AND CO PRODUCED BY H_2O AND/OR CO_2 REDUCTION IN MOLTEN CARBONATES: EFFECT OF GAS ENVIRONMENT AND HYDROXIDES

E. Gürbüz, V. Albin, V. Lair, A. Ringuedé and M. Cassir*

[1]*PSL Research University, Chimie Paristech-CNRS, Institut de Recherche de Chimie de Paris, 11 rue Pierre et Marie Curie, F-75231 Paris Cedex 05, France*

Abstract

Co-electrolysis of water and carbon dioxide in molten carbonates is nowadays a key issue in MCEC (molten carbonate electrolysis cell) and, reversely, for a better understanding of MCFC (molten carbonate fuel cell). The products of water and carbon dioxide reduction are the fuels that might be used in MCFC or other energy devices. The present study is dedicated to a thorough electrochemical investigation by voltammetric techniques (Cyclic Voltammetry CV or Linear Sweep Voltammetry LSV) at a Pt electrode of such fuels in Li_2CO_3-K_2CO_3 eutectic, under varied atmosphere conditions, including partial pressures of H_2O, CO_2, H_2 and Ar at 650 °C. The conditions of formation of soluble and/or adsorbed H_2 and CO are established together with qualitative thermodynamics information on the redox systems involved. C is only detected in very specific conditions. Knowing that hydroxides, produced in the conditions of MCEC and MCFC, have a significant role on the operation of such devices, an electrochemical analysis (CV and impedance measurements) of the effect of added amounts of hydroxides is developed for the first time, showing the enhancement of oxidation currents and the progressive increase in electrolyte conductivity.

Keywords: Molten Carbonate, Hydroxide additives, Electrochemistry, Conductivity, H_2O/CO_2 reduction.

* Corresponding author: michel.cassir@chimieparistech.psl.eu

I- Introduction

Water electrolysis and, more recently, H_2O and CO_2 co-electrolysis in molten carbonate electrolytes, MCEC (molten carbonate electrolysis cell), have attracted the interest of many research teams all over the world [1–19]. The complex reduction of CO_2 and H_2O has been addressed here and there, but there are still many major aspects to investigate thoroughly; in particular, when combining water and carbon dioxide in different ratios, including hydrogen and inert gas atmospheres. Moreover, the problem of CO_2 capture and purification/valorization by electrolysis in molten carbonates is becoming a major issue [20-24].

In parallel, the role of hydroxides, formed *in situ* or added, has been pointed out in different electrochemical devices involving molten carbonates: MCEC/MCFC (molten carbonate fuel cell), DCFC (direct carbon fuel cell) and MCFC/SOFC (solid oxide fuel cell) hybrid systems [25-31]. Thus, elucidation of the mechanisms involving the participation of hydroxides in molten carbonates is compulsory for optimizing the operation of the mentioned fuel cell/electrolyzer systems. Although some advances can be outlined on how molten hydroxides may act, in particular for MCFC application, no fundamental electrochemical study has ever been developed in the literature.

The direct analysis by voltammetric techniques of H_2O reduction in molten carbonates is difficult to identify thoroughly because of its proximity to the reduction limit (due to carbonates reduction), so we focussed specifically on the re-oxidation of the hydrogen produced. CO_2 reduction has been investigated in various papers. At a gold electrode, a mechanistic approach has been established, but gold can be partially passivated in carbonate media, which conduced us to use a Pt electrode where both H_2O and CO_2 reduction are close to the reduction limit [11,32]. Due to such considerations, we analysed specifically the re-oxidation process which corresponds to fuel oxidation in fuel cells.

Thus, the present study is dedicated in a first part to the systematic analysis by cyclic voltammetry or linear sweep voltammetry (LSV) of the oxidation behaviour of the products of CO_2 and H_2O reduction in varied gaseous atmospheres (CO_2, H_2O, H_2) in Li_2CO_3-K_2CO_3 eutectic using a Pt working electrode as in a recent publication [32]. The second part is a new approach dedicated to the influence of the addition of hydroxides in the molten carbonate eutectic through conductivity and cyclic voltammetry measurements.

II- Experimental

The electrochemical cell, an alumina cylindrical crucible placed in an alumina reactor, was described elsewhere [10, 37]. The electrolyte consists of Li_2CO_3 and K_2CO_3 (Sigma-Aldrich, purity > 98%) at the eutectic composition (62:38 mol%). Carbonate powders are dried at 120 °C for 24 h before heating at 650 °C under CO_2 (purity 99.99%). The system operates at atmospheric pressure. After any change in the atmosphere, a period of at least 4 h is left before analysis to ensure equilibrium. The 3-electrode setup was depicted previously [38]. A Pt plate was used as the working electrode (1*1 cm^2, AMTS, 99.95% purity). Prior to each measurement, the platinum plates were polished on SiC grinding paper P1200, P2400 and P4000 at 300 rpm and rinsed with Milli-Q purified water. An Autolab PGSTAT30 potentiostat controlled by either the GPES or NOVA software was used. Water pressure was obtained by bubbling the other gases in a temperature-controlled flask containing water.

Conductivity measurements were carried out by impedance spectroscopy with two gold planar electrodes set in parallel. The electrodes were similarly previously polished. Their dimensions are 1*1 cm^2, 0,5 mm thickness, and the distance between them is 2 cm. Measurements were carried out using the same potentiostat. The parameters used were the following: scanning frequencies between 0.1 and 10^5 Hz and 19 points per decade. Three different signal amplitudes were used: 5 mV, 50 mV and 100 mV. For each of them, the measurement was repeated at least 3 times to ensure repeatability.

III- Results and discussion

Effect of gas environment

In order to clearly identify the re-oxidation species of either H_2O or CO_2 reduction, the electrochemical experiments were carried out in gas atmospheres containing varied proportions of CO_2, H_2O and inert gas (Ar). The reactions of interest for co-electrolysis are given below:

$$H_2O + 2\,e^- \rightarrow H_2 + O^{2-} \quad (1)$$

$$CO_2 + 2\,e^- \rightarrow CO + O^{2-} \quad (2)$$

As a first step, we established a water environment (slightly diluted with Argon) and investigated the oxidation of hydrogen formed by H_2O reduction in the absence of CO_2. As observed in Fig. 1, the cyclic voltammogram reveals that water reduction at Pt electrode is difficult to analyze due to the lack of a well-defined wave, which is roughly the same at Au electrode. Nevertheless, two oxidation peaks appear during the reverse scan, one around -1.1 V *vs* Ag^+/Ag and the other close to -0.5 V vs Ag^+/Ag. These two peaks can be attributed to the oxidation of hydrogen proceeding from H_2O reduction, consistently with studies on H_2 oxidation in the literature, either at Au or Pt electrodes [31,39,40]. Indeed, no other reactant is present, and the cathodic reverse potential (-1.8 V *vs* Ag^+/Ag) is too low to consider a significant reduction of carbonates at a Pt electrode [32]. Besides, no C re-oxidation peak is observed, as well as no solid deposit can be identified at the electrode surface.

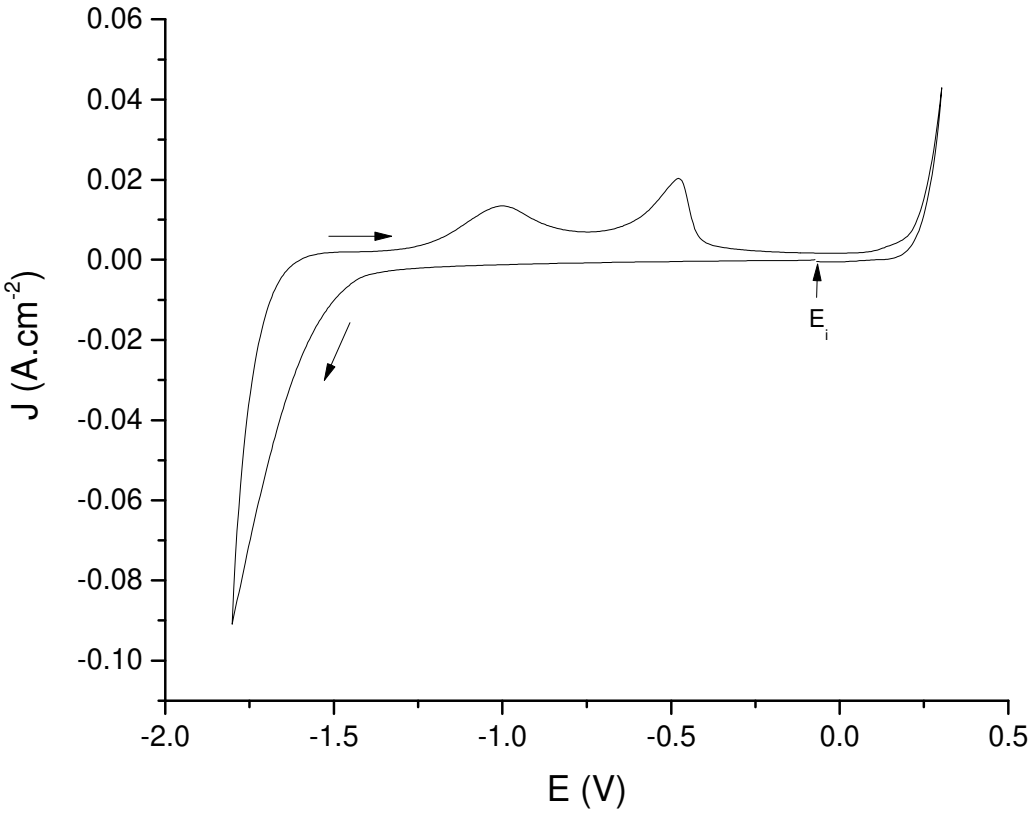

Fig. 1- Cyclic voltammogram at a Pt electrode in Li_2CO_3-K_2CO_3 under 70 mol% H_2O/30 mol% Ar at 650 °C. Scan rate 100 mV s^{-1}.

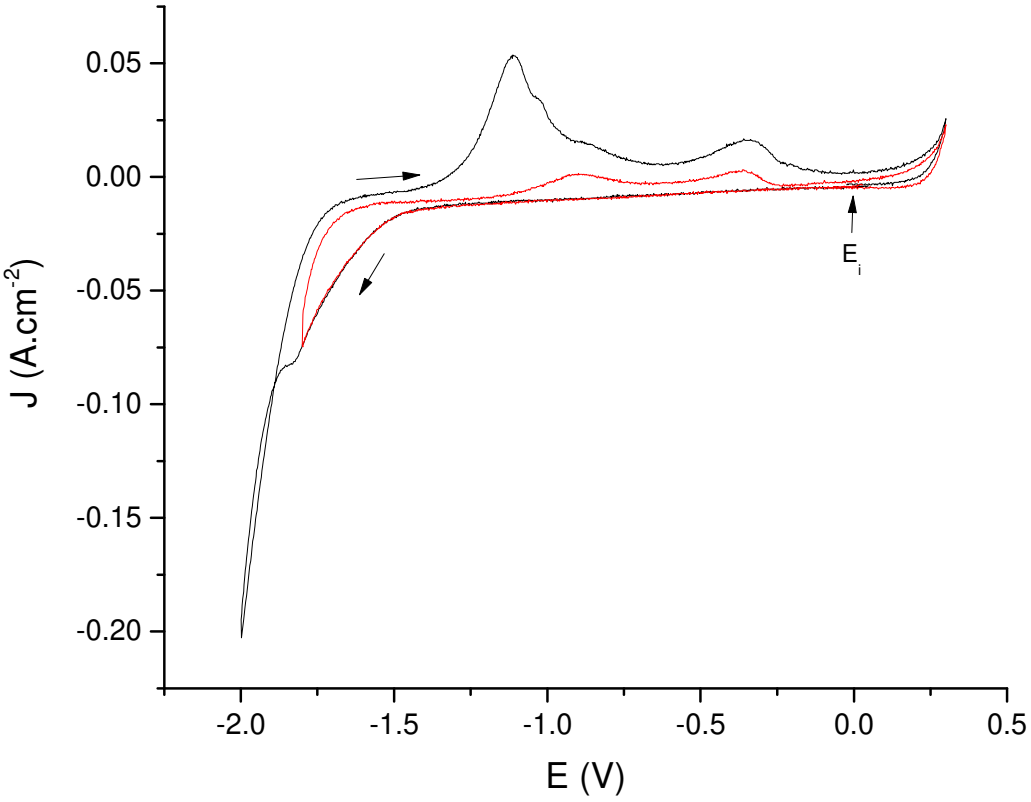

Fig. 2- Cyclic voltammogram at a Pt electrode in Li_2CO_3-K_2CO_3 under 100 mol% CO_2 at 650 °C. Scan rate 100 mV s^{-1}. Reverse potential at -1.8 V and -2 V vs Ag^+/Ag.

An example of carbon deposition, that tends to occur in oxobasic conditions but can happen in any case provided the reverse reduction potentials are negative enough, is given in Figure 2. At a reverse potential of -2 V *vs* Ag^+/Ag, one can observe the intersection of the forward and reverse scan indicating a solid deposit, with an intense peak visible at around -1.1 V *vs* Ag^+/Ag and a smaller one at -1.0 V *vs* Ag^+/Ag, which does not appear when the cathodic reverse potential is lower (red curve). This peak is attributed to the oxidation of C, in agreement with a previous study [41]. The doublet could be due to two different carbon oxidation phenomena at the Pt polycrystalline surface. At a reverse potential of -1.8 V *vs* Ag^+/Ag, the two peaks corresponding to C oxidation disappeared and only those relative to CO oxidation are visible (roughly here at -0.9 and -0.4 V and *vs* Ag^+/Ag). In previous studies in similar conditions at both Au or Pt electrodes, we have attributed such oxidation reactions to CO_{sol}/CO_{2sol} (both species dissolved) and CO_{ads}/CO_{2ads} (both adsorbed), respectively [11,32]. These systems are also visible when the reverse potential is -2 V *vs* Ag^+/Ag.

Besides, CO_2 reduction mechanism was also discussed in a previous article [32]. It was found that the mechanism in Li-K at 650 °C over Pt is as follows:

$$CO_2 + e^- \leftrightarrow CO_2^- \quad (3)$$

$$2\,CO_2^- \leftrightarrow CO + CO_3^{2-} \quad (4)$$

As dissolved species are considered for CO_2 reduction/ CO oxidation, it is also important to discuss speciation. It has been shown that both CO_2 and CO can form intermediates in molten carbonates [33, 34].

$$CO_2 + CO_3^{2-} \leftrightarrow C_2O_5^{2-} \quad (5)$$

$$CO + CO_3^{2-} \leftrightarrow C_2O_4^{2-} \quad (6)$$

The existence of the carbonite ion has also been suggested [35].

$$CO + CO_3^{2-} \leftrightarrow CO_2^{2-} + CO_2 \quad (7)$$

Even though CO_2 can be in a pyrocarbonate form around 20 % of the time, the ion only has a lifetime of some ps according to a recent molecular dynamics study [33]. Oxalates were found to be stable though reaction 6 did not spontaneously happen. Finally, a recent Raman investigation in Li-Na eutectic also showed CO_4^{2-} and HCO_4^- as active species under wet gas inlet [36]. As for the speciation of water itself, it will be discussed later in the hydroxide part.

Coming back to the oxidation peaks of Fig. 1, ascribed to hydrogen, a complementary study by Linear Sweep Voltammetry under hydrogen, as shown in Fig. 3 was conducted to thoroughly confirm this hypothesis. As can be seen, two peaks appear at around -1 and -0.5 V *vs* Ag^+/Ag (the second complex one being composed of three overlapped peaks), when only the oxidation sweep is investigated. When this same LSV experiment is conducted in the absence of hydrogen, no peaks are visible, and the same LSV can also be obtained over gold (not shown here), proving the oxidation phenomena to be unrelated to Pt. To better understand such phenomena, the scan rate was varied between 100 mV/s and 700 mV/s (in the case of the complex second peak, only the most intense component was analyzed). Figure 4 below reveals the evolution of both peak intensities and potentials with respect to scan rate.

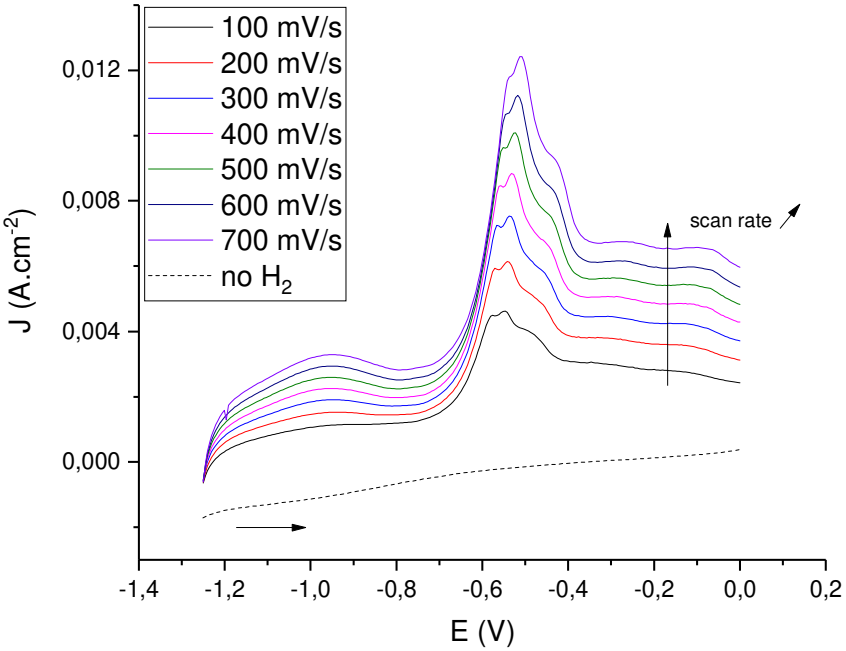

Fig. 3- LSV on a Pt electrode at various scan rates under 64 mol% H_2/20 mol % H_2O/16 mol % Ar. The baseline curve is drawn in the absence of H_2: 20 mol% H_2O/80 mol% Ar.

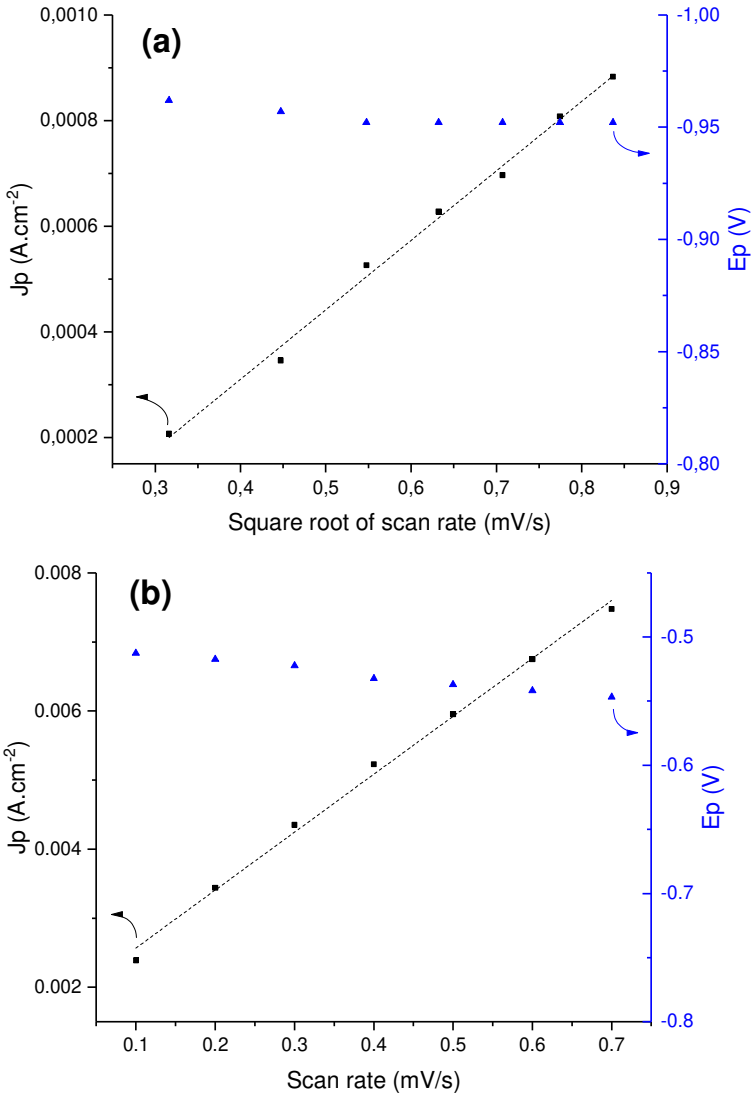

Fig. 4- Evolution of both oxidation peak potentials and currents with scan rate, with a the first (around -1 V vs Ag^+/Ag) and b the second peak (around -0.5 V vs Ag^+/Ag).

Both peak potentials present a slight variation with scan rate, indicating quasi-rapid phenomena. The first peak intensity presents a linear dependence on the square root of the scan rate ($R^2 = 0.994$), whereas the second peak intensity varies linearly with scan rate ($R^2 = 0.995$). Thus the first peak corresponds to a diffusion-limited process while the second is adsorption-controlled. Previous studies only assigned a peak around -1.1 V (over Au or Pt) to the oxidation of hydrogen, which would represent the first peak observed here [31, 40]. We observe two peaks related to this phenomenon, and the variation with scan rate seems to indicate that the first peak is oxidation of soluble H_2, and the second adsorbed H_2. The first oxidation peak, representing dissolved hydrogen, involves (as any electrochemical phenomenon) a very weak hydrogen intermediate adsorption, while the second one a strong

adsorption of hydrogen requiring a higher oxidation potential (additional energy). In fact, we can generalize to the three components around -0.5 V *vs* Ag^+/Ag: they are due to hydrogen adsorbed at three different hydrogen adsorption sites at the Pt polycrystalline surface.

From the obtained intensities, it appears that soluble H_2 is hard to visualize without reducing water first, in other words having H_2 directly formed in the vicinity of the electrode. Figure 5, where this peak is more intense, also highlights this point.

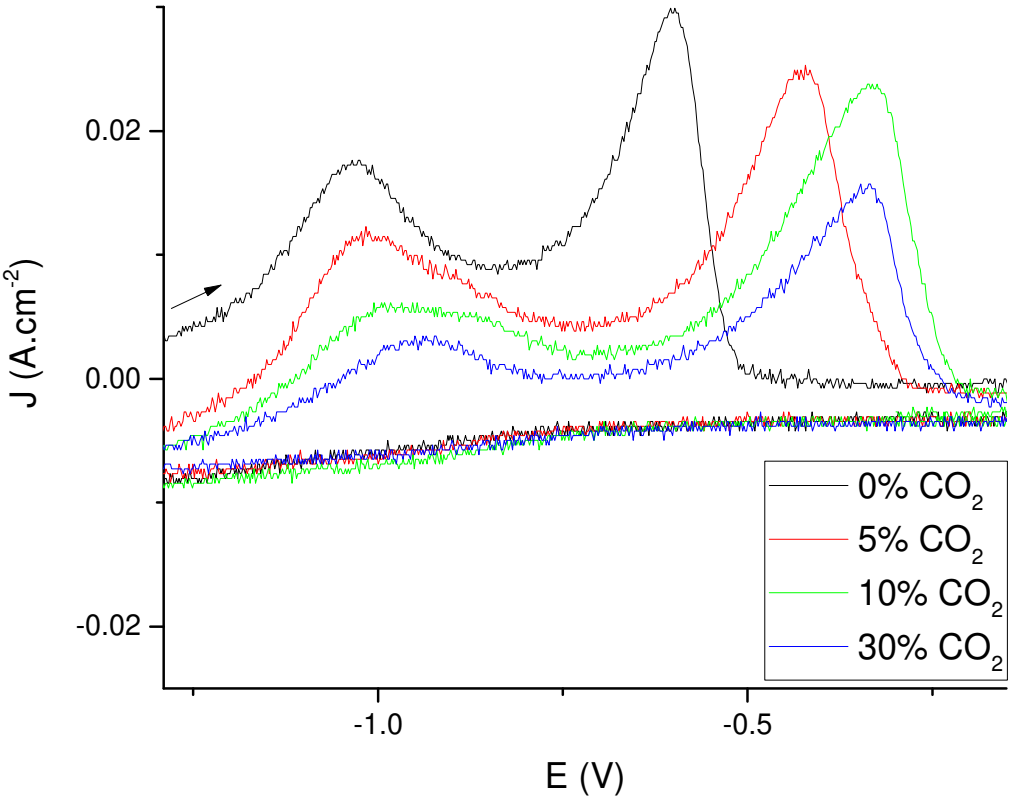

Fig. 5- Cyclic voltammogram reverse scans on a Pt electrode at 100 mV/s under 70 mol% H_2O and various amounts of CO_2.

Finally, a study under water and different amounts of CO_2 was conducted to visualize and separate CO and H_2 peaks. As soon as little amount of CO_2 is added, 2 peaks around -1 V *vs* Ag^+/Ag instead of one can be distinguished, a peak at a potential a little lower than -1 V *vs* Ag^+/Ag appearing. This peak has been reported in previous literature as oxidation of soluble CO [32].

Regarding the second oxidation peak (-0.5 V *vs* Ag^+/Ag), when 0 mol% CO_2 is present, it is undoubtedly the oxidation of H_2 that was previously seen. As soon as 5 mol% CO_2 is added, the peak seemingly shifts toward anodic potentials. This could either be simply due to the CO_2 pressure effect on potential, or the adsorbed CO oxidation also taking place. It is possible that both species compete for adsorption on the electrode surface.

As oxidation peaks found around -1 V *vs* Ag^+/Ag attributed to C, H_2 and CO are very close, studies become more complex and it is of high importance to carefully analyze the gas compositions, oxoacidity, potential domain in order to identify the suitable reactions. That is why studies in the literature focused either on CO_2 reduction (and subsequent C or CO oxidation) [32, 41] or H_2 oxidation [31], and it has been mentioned that cyclic voltammograms featuring oxidation of CO and oxidation of H_2 are qualitatively identical [40]. To gain better understanding of the reactions and their potentials, a potential-oxoacidity diagram can be considered. This type of diagram has been previously reported in the literature [10]. In our case, the calculations were done at 650 °C for the Li-K (62 :38 mol%) eutectic, which were the conditions used for electrochemical study, based on data from NIST-JANAF [42]. The resulting diagram is given in Figure 6.

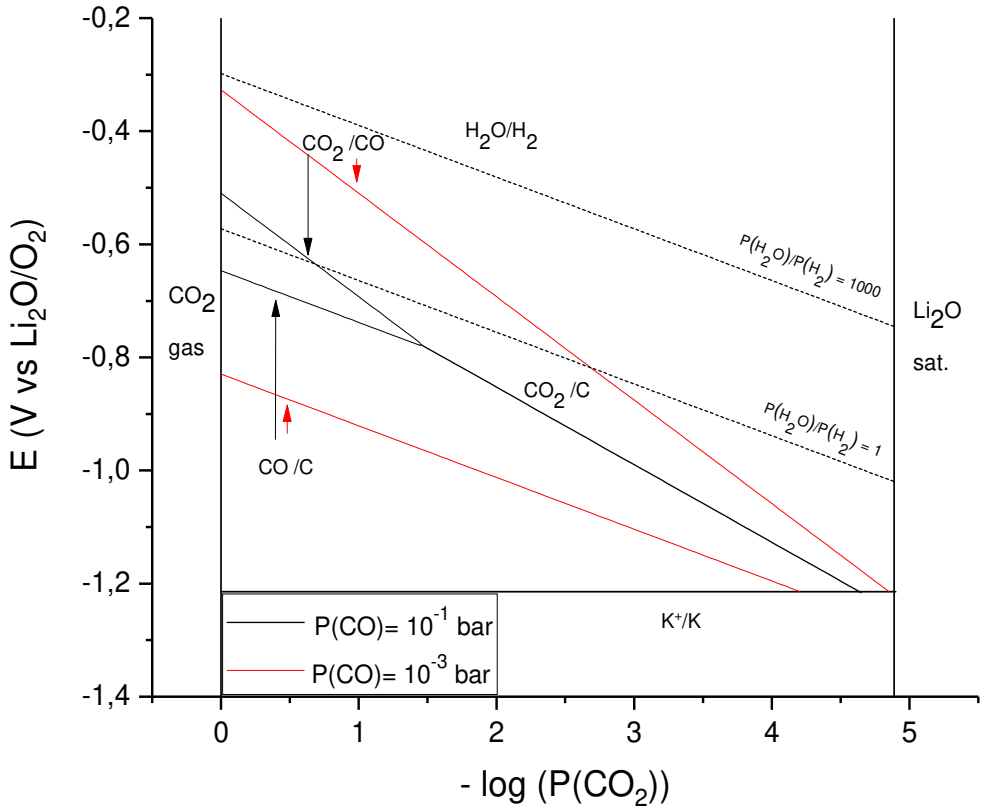

Fig. 6- Potential-oxoacidity diagram calculated for Li-K (62 :38 mol%) at 650 °C.

In oxoacidic conditions, it is possible to reduce CO_2 into CO and H_2O into H_2 at relatively low potentials. It is not possible to predict which species reduces first, as the potentials depend on the pressure of CO and H_2, that are most of the time unknown. However, both reactions should occur at potentials close to each other, barring kinetic issues. This indeed highlights the intriguing possibility of CO_2 and H_2O co-electrolysis into syngas. Oxoacidic conditions are more favorable thermodynamically, but in oxobasic conditions, both reactions are still possible, even though depending on the pressure of CO, reduction into carbon, which is undesirable in our case, could be more dominant.

At standard MCFC anode (MCEC cathode) conditions, 64 mol% H_2/16 mol% CO_2/20 mol% H_2O, water should thermodynamically reduce at -0.69 V vs Li_2O/O_2 and at this condition CO_2 will reduce beforehand unless the CO pressure is higher than 2.5 x 10^{-1} bar, which is unlikely considering no CO is fed.

Effect of the addition of hydroxides

Previous studies on the H_2 oxidation have led to three main mechanisms suggested by Ang and Sammels [43], Jewulski and Suski [44], and White and Twardoch [45, 46]. The first two mechanisms consider hydroxides as an intermediate species, while the last one suggests bicarbonates. Nishina *et al.* studied the H_2 oxidation in the Li-K eutectic at 650° C, at various metal electrodes, using cyclic voltammetry, electrochemical impedance spectroscopy and chronocoulometry [31]. They compared their findings to the three pathways proposed in the literature, only to conclude that the H_2 oxidation mechanism in their case was better described by the hydroxide mechanism suggested by Jewulski and Suski, which is:

$$H_2 \leftrightarrow 2\,H_{ads} \tag{8}$$

$$2\,\{H_{ads} + CO_3^{2-} \leftrightarrow OH^- + CO_2 + e^-\} \tag{9}$$

$$2\,OH^- + CO_2 \leftrightarrow H_2O + CO_3^{2-} \tag{10}$$

Applying the principle of microscopic reversibility, the water reduction mechanism in molten carbonates would be the exact opposite of the hydrogen oxidation one [3].

Another reason why hydroxides are an important species is that they are the associated oxobase of water, just as carbonates are the oxobase of CO_2. The autodissociation equilibrium is given in Reaction 11.

$$2\,OH^- \leftrightarrow O^{2-} + H_2O \tag{11}$$

In such case, they are likely to be present in the melt under water-containing atmospheres, as shown in the literature [3, 26, 27]. Indeed, even though it is generally accepted that water can form various dissolved species in molten carbonates, such as hydroxides and bicarbonates, it appears that the dominant species at 650 °C are hydroxides. Thermodynamical calculations relative to sodium hydroxide reaction into sodium bicarbonate have been carried out in the literature [3].

$$NaOH + CO_2 \leftrightarrow NaHCO_3 \tag{12}$$

They revealed through equilibrium concentration calculations that hydroxides are the dominant species above 550 °C, consistently with the proposed hydrogen oxidation mechanism above. Specifically, at 650 °C, the ratio [$NaHCO_3$]/[NaOH] was found to be 0.02 at a pressure of CO_2 equal to 0.5 atm.

Finally, it is known that molten hydroxides present high conductivity [47], so the effect of hydroxides was investigated both in terms of electrochemical reactivity and conductivity by adding different mol% of LiOH.

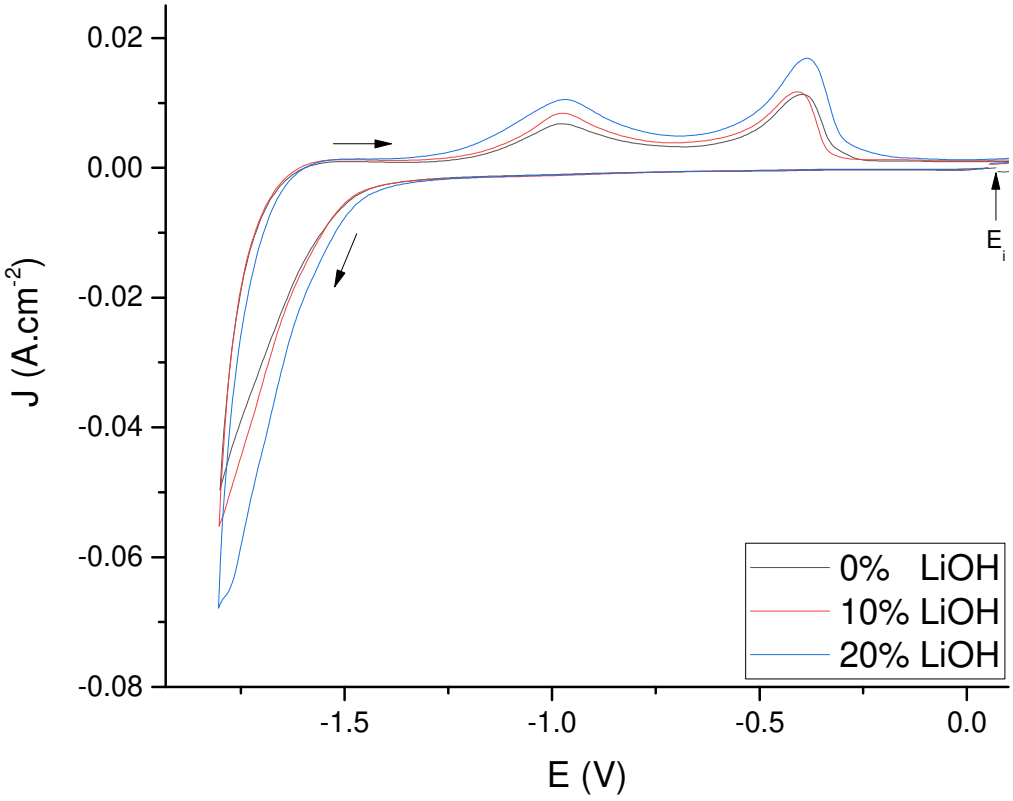

Fig. 7- Cyclic voltammograms on a Pt electrode at 100 mV/s under 70 mol% H_2O/15 mol% CO_2.

As seen in Figure 7, cyclic voltammetries carried out in the same conditions for various hydroxide contents under water reveal that currents are enhanced overall. Water reduction should indeed be favored with hydroxides present in the melt. In order to make sure the hydroxide ion is electroactive in our working conditions, an experiment was carried out under CO_2 and without water, shown in Figure 8. It is expected that hydroxides react according to the the following acid-base reaction:

$$2\,OH^- + CO_2 \leftrightarrow\ CO_3^{2-} +\ H_2O \qquad (13)$$

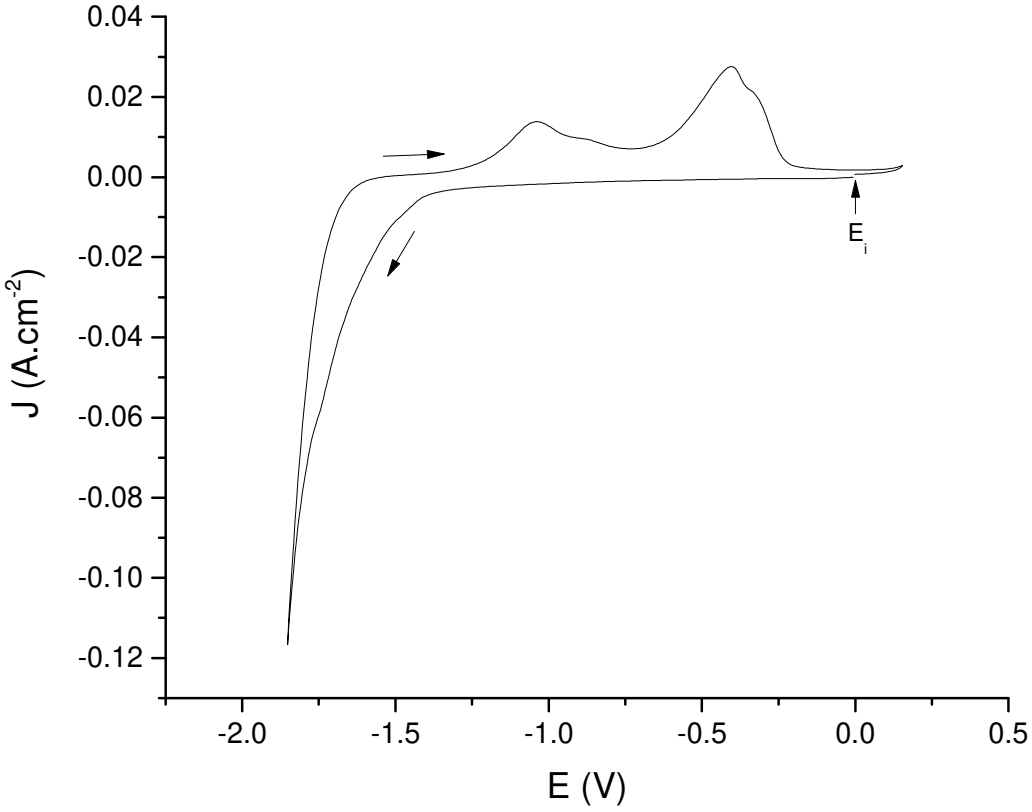

Fig. 8- Cyclic voltammogram on a Pt electrode at 100 mV/s under 100 mol% CO_2 right after 40 mol% LiOH addition.

Both oxidation peaks split into two: the peaks of hydrogen oxidation appear. The first appearing peak, around -1.1 V *vs* Ag^+/Ag, indeed depends on the square root of scan rate, and in these conditions carbon is not observed. This H_2 can only be obtained by reduction of hydroxides, proving they are electroactive in these conditions. Of course, water is to be provided for the hydroxides to remain stable, or Reaction 13 will occur in the presence of CO_2.

Finally, a possible influence of hydroxide addition on the conductivity was studied by EIS. It was found that the gas atmosphere had no significant influence on the conductivity. Its evolution with added hydroxide is reported in Figure 9.

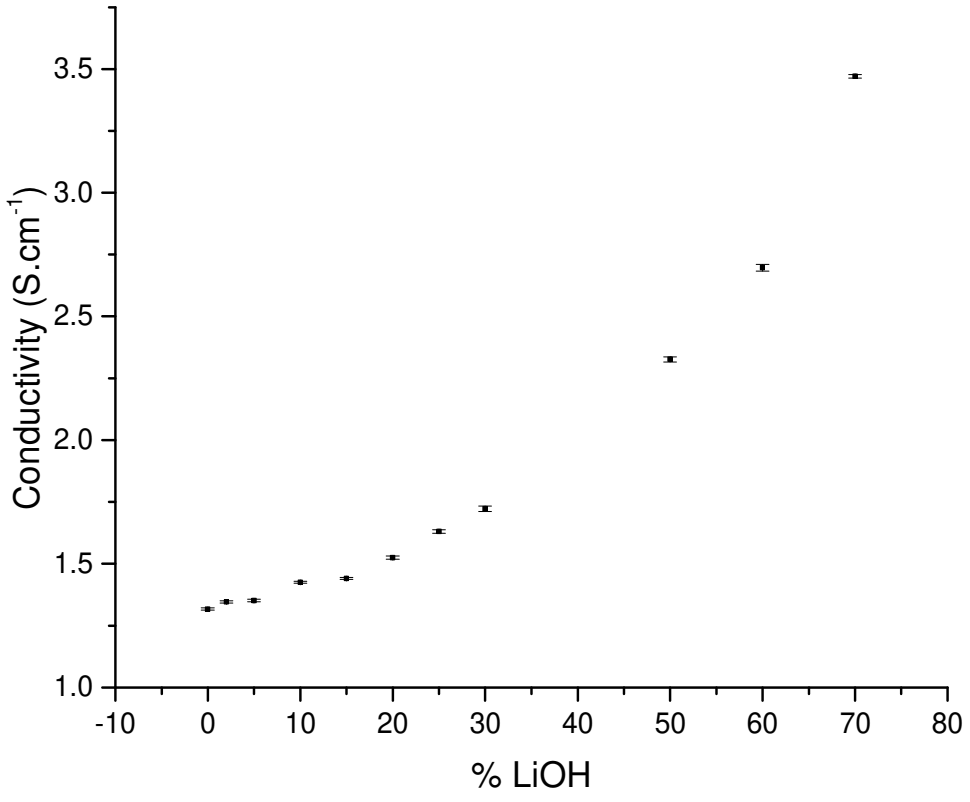

Fig. 9- Evolution of conductivity with added LiOH molar percentage at 650 °C.

The conductivity indeed increases with added LiOH content, thanks to the high mobility and low size of the lithium as well as hydroxide ions. The variation is even sharper for higher percentages. The Li-K eutectic without hydroxide features a conductivity of 1.3 $S.cm^{-1}$, while the highest value is obtained for Li-K + 70 mol% LiOH, around 3.5 $S.cm^{-1}$, which is close to conductivity values in pure LiOH at this temperature, extrapolated from the literature [48]. Already at a lower value of 10 mol% of LiOH, the conductivity reaches 1.45 $S.cm^{-1}$. Arrhenius law was also verified for each melt composition to check variation of the conductivity with the temperature. An example is given in Figure 10.

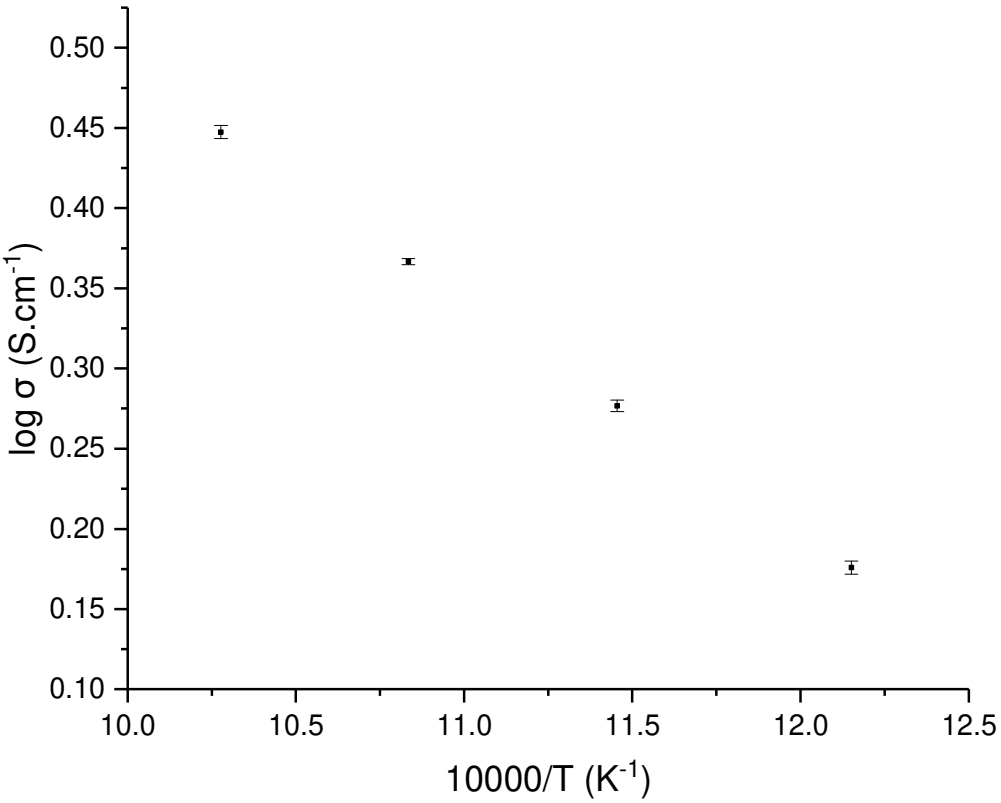

Fig. 10- Example of an Arrhenius plot for 50 mol% of added LiOH.

From the Arrhenius law, activation energies were calculated, and are reported in Figure 11.

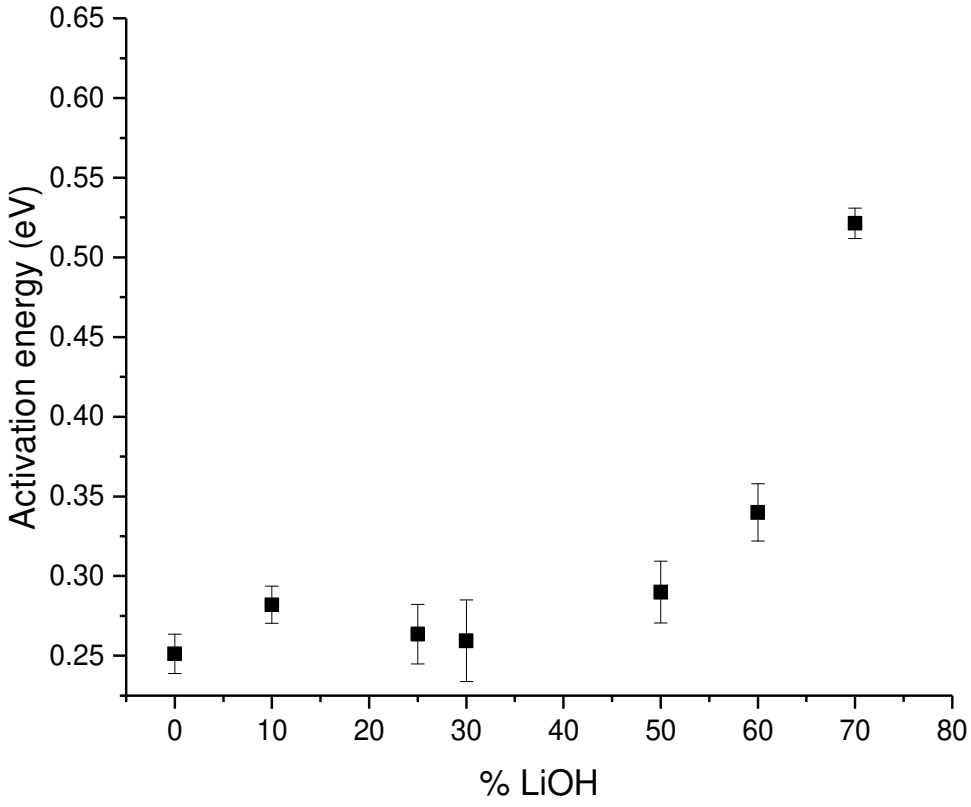

Fig. 11- Evolution of activation energies with added LiOH molar percentage.

Activation energies can be considered stable between 0 mol% and 30 mol% added LiOH, which is the zone of interest, at values of around 0.25 to 0.30 eV, which are consistent with previous literature on molten carbonates [49]. At higher percentages, an increase can be seen, with a value of 0.52 eV reached for 70 mol% LiOH. The melt is then composed mainly of hydroxides instead of carbonates. Two zones could be distinguished: at lower LiOH amounts, there is a conductivity increase with constant activation energy, while at higher percentages of added LiOH, both conductivity and activation energy steeply increase. The first zone could be due to the effect of the lithium ion addition, not changing the overall conduction mechanism, and an effect of the bigger hydroxide ion could be seen in the second zone, where activation energy is much greater.

It is indeed best to limit addition of hydroxides to a reasonable amount, less than 30 mol%, to not deeply alter the base melt of eutectic Li-K (62:38 mol%) while enhancing conductivity (up to 1.72 $S.cm^{-1}$ for 30 mol% added LiOH) and water reduction. This paves the way for a

direct application of a mixed carbonate/hydroxide electrolyte in the MCFC/MCEC system: not only would it be helpful both in fuel cell and electrolysis mode due to increased conductivity, but specifically in MCEC mode water reduction would be favored.

IV- Conclusion

According to our electrochemical investigation at a Pt working electrode, including CV and LSV, H_2 and/or CO are produced through H_2O and/or CO_2 reduction in molten Li_2CO_3-K_2CO_3 at 650 °C in atmospheres containing different proportions of CO_2, H_2O, H_2 and Ar. Both fuels are detected in a soluble or adsorbed form: this is confirmed by the linear evolution of the oxidation peaks with respect to $v^{1/2}$ or v, respectively for diffusion- or adsorption-controlled processes. C is only detected species when the cathodic potential is very negative provoking the reduction of carbonate ions into C. We also confirmed that the oxidation of CO occurs in two steps under CO_2-rich atmospheres. In water-rich atmospheres, both oxidation of soluble H_2 and CO are overlapped for low ratios of CO_2; at 30% of CO_2, only CO oxidation can be observed. Under hydrogen-rich atmospheres without CO_2, scanning directly towards anodic potentials allows to detect a low-intensity oxidation peak due to soluble H_2 and a high-intensity oxidation peak due to adsorbed H_2; the latest is decomposed into several peaks with close-by potentials, indicating that hydrogen is adsorbed on different adsorption sites on the polycrystalline working Pt electrode. In water-rich atmospheres, addition of hydroxides enhances the oxidation peaks due to H_2, showing that the presence of hydroxides favors H_2O reduction. Even under CO_2 atmosphere, hydroxides react with CO_2 to produce water: H_2 and CO peaks are overlapped. The increase in the conductivity of Li_2CO_3-K_2CO_3 with progressive addition of hydroxides is clearly evidenced by EIS: the activation energy deduced from Arrhenius plots is constant up to 30% of added LiOH. Thus there is a significant effect of hydroxides both on the electrochemical oxidation reaction and on the conductivity of the electrolyte. This confirms the role of hydroxides produced *in situ* in MCFC operation conditions and opens the possibility of using a molten carbonate eutectic containing hydroxides in the MCFC/MCEC system, which presents the advantage of relying on a mature MCFC technology and the combination of CO_2 capture with energy generation. The direct use of molten hydroxide melts in fuel cell/electrolyzer applications, scarcely mentioned in the literature, would require further studies and scale-up experiments.

Acknowledgments

This work was supported by the French programs PLANEX ANR-11-EQPX-0-01 and ANR MCEC 17-CE05-0025-01.

References

[1] P.K. Lorenz, G.J. Janz, Electrolysis of molten carbonates: anodic and cathodic gas-evolving reactions, Electrochim. Acta 15 (1970) 1025–1035. https://doi.org/10.1016/0013-4686(70)80042-1.

[2] V. Kaplan, E. Wachtel, K. Gartsman, Y. Feldman, I. Lubomirsky, Conversion of CO_2 to CO by Electrolysis of Molten Lithium Carbonate, J. Electrochem. Soc. 157 (2010) B552. https://doi.org/10.1149/1.3308596.

[3] S. Frangini, C. Felici, P. Tarquini, A Novel Process for Solar Hydrogen Production Based on Water Electrolysis in Alkali Molten Carbonates, ECS Transactions 61 (2014) 13–25. https://doi.org/10.1149/06122.0013ecst.

[4] L. Hu, I. Rexed, G. Lindbergh, C. Lagergren, Electrochemical performance of reversible molten carbonate fuel cells, Int. J. Hydrogen Energ. 39 (2014) 12323–12329. https://doi.org/10.1016/j.ijhydene.2014.02.144.

[5] L. Hu, G. Lindbergh, C. Lagergren, Performance and Durability of the Molten Carbonate Electrolysis Cell and the Reversible Molten Carbonate Fuel Cell, J. Phys. Chem. C. 120 (2016) 13427–13433. https://doi.org/10.1021/acs.jpcc.6b04417.

[6] L. Hu, G. Lindbergh, C. Lagergren, Electrode Kinetics of the Ni Porous Electrode for Hydrogen Production in a Molten Carbonate Electrolysis Cell (MCEC), J. Electrochem. Soc. 162 (2015) F1020–F1028. https://doi.org/10.1149/2.0491509jes.

[7] L. Hu, G. Lindbergh, C. Lagergren, Electrode kinetics of the NiO porous electrode for oxygen production in the molten carbonate electrolysis cell (MCEC), Faraday Discuss. 182 (2015) 493–509. https://doi.org/10.1039/C5FD00011D.

[8] D. Chery, V. Lair, M. Cassir, Overview on CO_2 Valorization: Challenge of Molten Carbonates, Front. Energy Res. 3 (2015). https://doi.org/10.3389/fenrg.2015.00043.

[9] D. Chery, V. Albin, V. Lair, M. Cassir, Thermodynamic and experimental approach of electrochemical reduction of CO_2 in molten carbonates, Int. J. Hydrogen Energ. 39 (2014) 12330–12339. https://doi.org/10.1016/j.ijhydene.2014.03.113.

[10] D. Chery, V. Lair, M. Cassir, CO_2 electrochemical reduction into CO or C in molten

carbonates: a thermodynamic point of view, Electrochim. Acta 160 (2015) 74–81. https://doi.org/10.1016/j.electacta.2015.01.216.

[11] D. Chery, V. Albin, A. Meléndez-Ceballos, V. Lair, M. Cassir, Mechanistic approach of the electrochemical reduction of CO_2 into CO at a gold electrode in molten carbonates by cyclic voltammetry, Int. J. Hydrogen Energ. 41 (2016) 18706–18712. https://doi.org/10.1016/j.ijhydene.2016.06.094.

[12] H. Meskine, E. Gürbüz, V. Albin, A. Meléndez-Ceballos, M. Cassir, A. Ringuedé, V. Lair, CO_2 electrolysis in a reversible molten carbonate fuel cell: Online chromatographic detection of CO, Int. J. Hydrogen Energ. 46 (2021) 14913–14921. https://doi.org/10.1016/j.ijhydene.2020.08.028.

[13] J.P. Perez-Trujillo, F. Elizalde-Blancas, M. Della Pietra, S.J. McPhail, A numerical and experimental comparison of a single reversible molten carbonate cell operating in fuel cell mode and electrolysis mode, Appl. Energ. 226 (2018) 1037–1055. https://doi.org/10.1016/j.apenergy.2018.05.121.

[14] J.P. Pérez-Trujillo, F. Elizalde-Blancas, S.J. McPhail, M. Della Pietra, B. Bosio, Preliminary theoretical and experimental analysis of a Molten Carbonate Fuel Cell operating in reversible mode, Appl. Energ. 263 (2020) 114630. https://doi.org/10.1016/j.apenergy.2020.114630.

[15] H. Wu, D. Ji, L. Li, D. Yuan, Y. Zhu, B. Wang, Z. Zhang, S. Licht, A New Technology for Efficient, High Yield Carbon Dioxide and Water Transformation to Methane by Electrolysis in Molten Salts. Adv. Mater. Technol. 1 (2016) 1600092. doi:10.1002/admt.201600092.

[16] Y. Liu, D. Yuan, D. Ji, Z. Li, Z. Zhang, B. Wang, H. Wu, Syngas production: diverse H_2/CO range by regulating carbonates electrolyte composition from CO_2 /H_2O via co-electrolysis in eutectic molten salts, RSC Adv. 7 (2017) 52414–52422. https://doi.org/10.1039/C7RA07320H.

[17] D. Ji, Z. Li, W. Li, D. Yuan, Y. Wang, Y. Yu, H. Wu, The optimization of electrolyte composition for CH_4 and H_2 generation via CO_2/H_2O co-electrolysis in eutectic molten salts, Int. J. Hydrogen Energ. 44 (2019) 5082–5089. https://doi.org/10.1016/j.ijhydene.2018.09.089.

[18] Z. Li, Y. Yu, W. Li, G. Wang, L. Peng, J. Li, D. Gu, D. Yuan, H. Wu, Carbon dioxide electrolysis and carbon deposition in alkaline-earth-carbonate-included molten salts electrolyzer, New J. Chem. 42 (2018) 15663–15670. https://doi.org/10.1039/C8NJ02965B.

[19] S. Licht, S. Liu, B. Cui, J. Lau, L. Hu, J. Stuart, B. Wang, O. El-Ghazawi, F.-F. Li, Comparison of Alternative Molten Electrolytes for Water Splitting to Generate Hydrogen Fuel, J. Electrochem. Soc. 163 (2016) F1162. https://doi.org/10.1149/2.0561610jes.

[20] A. Meléndez-Ceballos, E. Gürbüz, A. Brouzgou, V. Albin, A. Ringuedé, V. Lair, M. Cassir, Input on the Measurement and Comprehension of CO_2 Solubility in Molten Alkali Carbonates in View of Its Valorization, J. Electrochem. Soc. 167 (2020) 064504. https://doi.org/10.1149/1945-7111/ab7ce1.

[21] Intergovernmental panel on climate change. In: Metz B, editor. IPCC Special report on carbon dioxide capture and storage. Cambridge: Cambridge University Press, for the Intergovernmental Panel on Climate Change; 2005.

[22] M. Cassir, S.J. McPhail, A. Moreno, Strategies and new developments in the field of molten carbonates and high-temperature fuel cells in the carbon cycle, Int. J. Hydrogen Energ. 37 (2012) 19345–19350. https://doi.org/10.1016/j.ijhydene.2011.11.006.

[23] Fuel Cell Energy, Carbon Capture with Direct Fuel Cell Carbonate Powerplants. http://www.sccs.org.uk/images/events/2017/8-Carbon-Capture-with-DFC-Fuel-Cells-022117a.pdf [Accessed June 27, 2019].

[24] Fuel cell energy announces new carbon capture project with drax power station. http://www.globenewswire.com [Accessed June 27, 2019].

[25] E. Gürbüz, E. Grépin, A. Ringuedé, V. Lair, M. Cassir, Significance of Molten Hydroxides With or Without Molten Carbonates in High-Temperature Electrochemical Devices, Front. Energy Res. 9 (2021). https://doi.org/10.3389/fenrg.2021.666165.

[26] J. Rosen, T. Geary, A. Hilmi, R. Blanco-Gutierrez, C.-Y. Yuh, C.S. Pereira, L. Han, R.A. Johnson, C.A. Willman, H. Ghezel-Ayagh, T.A. Barckholtz, Molten Carbonate Fuel Cell Performance for CO2 Capture from Natural Gas Combined Cycle Flue Gas, J. Electrochem. Soc. 167 (2020) 064505. https://doi.org/10.1149/1945-7111/ab7a9f.

[27] E. Audasso, B. Bosio, D. Bove, E. Arato, T. Barckholtz, G. Kiss, J. Rosen, H. Elsen, R.B. Gutierrez, L. Han, T. Geary, C. Willman, A. Hilmi, C.Y. Yuh, H. Ghezel-Ayagh, New, Dual-Anion Mechanism for Molten Carbonate Fuel Cells Working as Carbon Capture Devices, J. Electrochem. Soc. 167 (2020) 084504. https://doi.org/10.1149/1945-7111/ab8979.

[28] E. Arato, E. Audasso, L. Barelli, B. Bosio, G. Discepoli, Kinetic modelling of molten

carbonate fuel cells: Effects of cathode water and electrode materials. J. Power Sources 330 (2016) 18–27. https://doi.org/10.1016/j.jpowsour.2016.08.123.

[29] E. Audasso, L. Barelli, G. Bidini, B. Bosio, and G. Discepoli, Molten Carbonate Fuel Cell performance analysis varying cathode operating conditions for carbon capture applications. J. Power Sources 348 (2017) 118–129. https://doi.org/10.1016/j.jpowsour.2017.02.081.

[30] A. Evans, W. Xing, T. Norby, Electromotive Force (emf) Determination of Transport Numbers for Native and Foreign Ions in Molten Alkali Metal Carbonates. J. Electrochem. Soc. 162 (2015) F1135–F1143. https://doi.org/10.1149/2.0121510jes.

[31] T. Nishina, M. Takahashi, I. Uchida, Gas electrode reactions in molten carbonate media: IV. Electrode Kinetics and Mechanism of Hydrogen Oxidation in (Li+K)CO_3 Eutectic. J. Electrochem. Soc. 137 (1990) 1112–1121. https://doi.org/10.1149/1.2086612.

[32] H. Meskine, V. Albin, M. Cassir, A. Ringuedé, V. Lair, Electrochemical investigations on CO_2 reduction mechanism in molten carbonates in view of H_2O/CO_2 co-electrolysis, Int. J. Hydrogen Energ. 46 (2021) 14944–14952. https://doi.org/10.1016/j.ijhydene.2020.07.008.

[33] A. Carof, F.-X. Coudert, D. Corradini, D. Lesnicki, E. Desmaele, R. Vuilleumier, Carbon species solvated in molten carbonate electrolyser cell from first-principles simulations, Int. J. Hydrogen Energ. 46 (2021) 15008–15023. https://doi.org/10.26434/chemrxiv.12271841.

[34] D. Corradini, F.-X. Coudert, R. Vuilleumier, Carbon dioxide transport in molten calcium carbonate occurs through an oxo-Grotthuss mechanism via a pyrocarbonate anion, Nature Chem. 8 (2016) 454–460. https://doi.org/10.1038/nchem.2450.

[35] P. Claes, B. Thirion, J. Glibert, Solubility of CO_2 in the molten Na_2CO_3-K_2CO_3 (42 mol %) eutectic mixture at 800°C, Electrochim. Acta 41 (1996) 141−146. https://doi.org/10.1016/0013-4686(95)00278-M.

[36] P. Zhang, T. Wu, K. Huang, Identification of Active Surface Species in Molten Carbonates Using in situ Raman Spectroscopy, Front. Energy Res. 9 (2021). https://doi.org/10.3389/fenrg.2021.653527.

[37] A. Meléndez-Ceballos, V. Albin, C. Crapart, A. Ringuedé, V. Lair, M. Cassir. Influence of Cs and Rb additions in Li-K and Li-Na molten carbonates on the

behaviour of a commercial MCFC nickel cathode, Int. J. Hydrogen Energ. 42 (2017) 1853-1858. https://doi.org/10.1016/j.ijhydene.2016.09.118.

[38] M. Cassir, G. Moutiers, J. Devynck, Stability and Characterization of Oxygen Species in Alkali Molten Carbonate: A Thermodynamic and Electrochemical Approach, J. Electrochem. Soc. 140 (1993) 3114–3123. https://doi.org/10.1149/1.2220995.

[39] M. Cassir, V. Chauvaut, A. Alfarra, V. Albin, Study of cerium species in molten Li_2CO_3-Na_2CO_3 in the conditions used in molten carbonate fuel cells. Part II: potentiometric & voltammetric behavior. J. Applied Electrochem. 30 (2000) 1415-1420. https://doi.org/10.1023/A:1026555502949.

[40] R. Weewer, Ph.D. Thesis, TU Delft, 1991.

[41] H.V. Ijije, R.C. Lawrence, N.J. Siambun, S.M. Jeong, D.A. Jewell, D. Hu, G.Z. Chen, Electro-deposition and re-oxidation of carbon in carbonate-containing molten salts. Faraday Discuss. 172 (2014) 105-116. https://doi.org/10.1039/C4FD00046C.

[42] M. W. Chase, in: NIST-JANAF Thermochemical Tables. 4th ed. J. Phys. Chem. Ref. Data; 1998. Monograph No. 9.

[43] P.G.P. Ang, A.F. Sammells, Influence of Electrolyte Composition on Electrode Kinetics in the Molten Carbonate Fuel Cell, J. Electrochem. Soc. 127 (1980) 1287. https://doi.org/10.1149/1.2129873.

[44] J. Jewulski, L. Suski, Model of the isotropic anode in the molten carbonate fuel cell, J. Appl. Electrochem. 14 (1984) 135–143. https://doi.org/10.1007/BF00618732.

[45] S.H. White, U.M. Twardoch, The electrochemical behaviour of solutions of molten ternary alkali carbonate mixture equilibrated with carbon dioxide-water mixtures at 460°C, Electrochim. Acta 29 (1984) 349–359. https://doi.org/10.1016/0013-4686(84)87074-7.

[46] S.H. White, U.M. Twardoch, The Behavior of Water in Molten Salts, J. Electrochem. Soc. 134 (1987) 1080. https://doi.org/10.1149/1.2100620.

[47] S. Zecevic, E. M. Patton, P. Parhami, Direct Carbon Fuel Cell With Molten Hydroxide Electrolyte, in 2nd International Conference on Fuel Cell Science, Engineering and Technology, Rochester, New York, USA (2004) 387–394. https://doi.org/10.1115/FUELCELL2004-2496.

[48] P. Claes, J. Gilbert, Electrical Conductivity and Specific Mass of the Molten LiOH-$LiNO_3$, NaOH-$NaNO_3$, and KOH-KNO_3 Mixtures, J. Electrochem. Soc. 132 (1985) 6. https://doi.org/10.1149/1.2113973.

[49] V. Lair, V. Albin, A. Ringuedé, M. Cassir, Theoretical predictions vs. experimental measurements of the electrical conductivity of molten Li_2CO_3–K_2CO_3 modified by additives, Int. J. Hydrogen Energ. 37 (2012) 19357–19364. https://doi.org/10.1016/j.ijhydene.2011.09.153.